

# Universality in the Onset of Super-Diffusion in Levy Walks

Asaf Miron

*Department of Physics of Complex Systems, Weizmann Institute of Science, Rehovot 7610001, Israel*

Anomalous dynamics in which local perturbations spread faster than diffusion are ubiquitously observed in the long-time behavior of a wide variety of systems. Here, the manner by which such systems evolve towards their asymptotic superdiffusive behavior is explored using the 1d Levy walk of order  $1 < \beta < 2$ . The approach towards superdiffusion, as captured by the leading correction to the asymptotic behavior, is shown to remarkably undergo a transition as  $\beta$  crosses the critical value  $\beta_c = 3/2$ . Above  $\beta_c$ , this correction scales as  $|x| \sim t^{1/2}$ , describing simple diffusion. However, below  $\beta_c$  it is instead found to remain superdiffusive, scaling as  $|x| \sim t^{1/(2\beta-1)}$ . This transition is shown to be independent of the precise model details and is thus argued to be universal.

*Introduction* - The Levy walk has proven to be an effective instrument for modeling a vast number of physical and biological phenomena in which transport is faster than diffusion. For example, it has been shown to successfully reproduce the peculiar scaling exhibited by chaotic and turbulent systems [1, 2], the super-diffusive spreading of perturbations and associated anomalous transport properties of low-dimensional many-body systems [3–8], anomalous tagged particle dynamics in disordered media [9, 10], the spatial evolution of trapped ions and atoms in optical lattices [11–13] and even the behavior exhibited by living matter [14], on both microscopic [15–17] and macroscopic scales [18, 19].

In 1d, the Levy walk describes particles whose evolution consists of many random excursions on the infinite line. In each such excursion the walker draws a random direction in which it walks, at a constant velocity of magnitude  $v$ , for a random duration  $u$  [6, 20, 21]. The “walk time”  $u$  is drawn from a heavy-tailed distribution  $\phi(u)$  which behaves as  $\propto 1/u^{1+\beta}$  for large  $u$ , with  $\beta$  called the “order” of the Levy walk. The Levy walk is well known to exhibit superdiffusive behavior in the regime  $1 < \beta < 2$  [21]. There, the divergence of all but the zeroth and first moments of  $\phi(u)$  profoundly affects the walker’s motion: While the average walk duration is finite, the second moment’s divergence implies that the walker has a chance to persist in very long excursions. This is manifested in the probability density  $P(x, t)$  of finding the walker inside the space interval  $(x, x + \mathbf{d}x)$  at time  $t$ , given it began its motion at the origin. For long times and large distances  $P(x, t)$  is dominated by unusually long excursions, leading to the asymptotic superdiffusive scaling form  $P_0(x, t) = t^{-1/\beta} f(t^{-1/\beta} |x|)$ , where  $f$  is a known function of the scaling variable  $t^{-1/\beta} |x|$  [21–24]. We shall henceforth use the subscript 0 to refer to the leading asymptotic scaling solution.

This hallmark result has paved the way for employing the Levy walk to model the superdiffusive transport behavior observed in experiments and numerical simulations of numerous systems, across a broad range of sci-

entific disciplines, of which several examples have been mentioned above. Yet experimental setups and numerical simulations alike are inherently confined to finite laboratories, data sets, computer memory and graduate program’s duration. Superdiffusive behavior and a convincing connection to the Levy walk model may consequently be hard to characterize correctly and convincingly in cases where the asymptotic limit is hard to reach in practice [3, 25–29]. An interesting question which naturally arises in this context is: “How do superdiffusive systems approach their limiting asymptotic behavior?”. In particular, “Do superdiffusive dynamics possess any universal features which become visible *before* the strictly asymptotic regime is reached?”.

This letter studies the onset of superdiffusion in the 1d Levy walk of order  $1 < \beta < 2$ . Specifically, the leading correction to the asymptotic probability density  $P_0(x, t)$ , which describes the approach of  $P(x, t)$  towards its asymptotic form, is computed and analyzed. A transition is reported as  $\beta$  crosses the critical value  $\beta_c = 3/2$ . For  $\beta > \beta_c$ , the correction scales diffusively as  $|x| \propto t^{1/2}$  while for  $\beta < \beta_c$  it remains super-diffusive, scaling as  $|x| \propto t^{1/(2\beta-1)}$ . This transition is shown to depend only on the tail behavior of  $\phi(u)$  and is thus argued to be universal.

*The Model* - The Levy walk of order  $\beta$  describes particles moving at a fixed velocity  $v$  on the infinite line. Their motion consists of many random excursions, each in a random direction and lasting a random duration  $u$  drawn from the distribution

$$\phi(u) = \beta t_0^\beta \frac{\theta[u - t_0]}{u^{1+\beta}}. \quad (1)$$

The Heaviside step function  $\theta(x)$  keeps  $\phi(u)$  normalizable at  $u = 0$  by imposing a cutoff below a minimal walk time  $t_0 > 0$ .

Figure 1 presents examples of a single walker trajectory for different values of  $\beta$ , qualitatively illustrating the difference between simple Brownian motion and the Levy walk for two different values of  $\beta$ . For  $\beta > 2$ ,

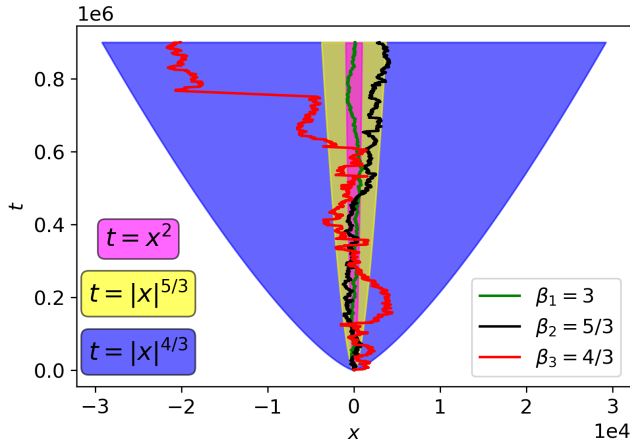


Figure 1. Illustrative examples of a single Levy walk trajectory for three different values of  $\beta$ , alongside the corresponding asymptotic scaling regimes. For  $\beta > 2$  the Levy walk effectively reduces to Brownian motion, as depicted by the green trajectory for  $\beta_1 = 3$  which is contained within the diffusive scaling regime  $t = x^2$  (magenta). The black trajectory for  $\beta_2 = 5/3$ , contained within the superdiffusive scaling regime  $t = |x|^{5/3}$  (yellow), appears to consist of diffusive motion that is occasionally interrupted by long bouts of “ballistic” motion. Such ballistic bouts become more frequent, pronounced and erratic in the red trajectory for  $\beta_3 = 4/3$ , confined to the superdiffusive scaling regime  $t = |x|^{4/3}$ .

both the first and second moments of  $\phi(u)$  are finite and the Levy walk effectively reduces to Brownian motion [21, 22]. For  $1 < \beta < 2$ , which corresponds to the superdiffusive regime considered in this letter, the average walk time remains finite but the second moment diverges, occasionally giving rise to very long excursions which grow increasingly more probable as  $\beta$  approaches 1. We hereafter restrict our discussion to the range  $1 < \beta < 2$ .

The probability of finding the walker inside the interval  $(x, x + \mathbf{d}x)$  at time  $t$  for an initial condition  $P(x, 0) = \delta(x)$  satisfies the integral equation [6, 21]

$$P(x, t) = \frac{\psi(t)}{2} \delta(|x| - vt) + \frac{1}{2} \int_0^t \mathbf{d}u \phi(u) [P(x - vu, t - u) + P(x + vu, t - u)], \quad (2)$$

where  $\psi(u)$  is the probability of drawing a walk-time greater than  $u$ , i.e.

$$\psi(u) = \int_u^\infty \mathbf{d}w \phi(w) = 1 - \theta[u - t_0] \left(1 - (t_0/u)^\beta\right). \quad (3)$$

The first line on the right hand side of Eq. (2) describes the walker’s probability to cross position  $x$  at time  $t$  during its initial excursion and the second line describes its probability of drawing a walk time  $u$  which leads it to position  $x$  at time  $t$ , given that the previous excursion had ended at position  $x \pm vu$  at time  $t - u$ .

Following a Fourier-Laplace transform (see Sec. I of the SM), Eq. (2) becomes

$$\tilde{P}(k, s) = \frac{\tilde{\psi}(s - ivk) + \tilde{\psi}(s + ivk)}{2 - \tilde{\phi}(s - ivk) - \tilde{\phi}(s + ivk)}. \quad (4)$$

Here  $\tilde{P}(k, s) = \int_0^\infty \mathbf{d}t e^{-st} \hat{P}(k, t)$  is the Laplace transform of the Fourier transformed probability density  $\hat{P}(k, t) = \int_{-\infty}^\infty \mathbf{d}x e^{-ikx} P(x, t)$ ,  $\tilde{\phi}(s \pm ivk)$  and  $\tilde{\psi}(s \pm ivk)$  are the respective Fourier-Laplace transforms of  $\phi(t)$  and  $\psi(t)$ , and  $(k, s)$  are the respective Fourier/Laplace conjugates of  $(x, t)$ .

*Main Results* - The following results, as well as the forthcoming analysis, are presented in Fourier space since only there does the probability density admit a closed form. The leading correction to the asymptotic probability density  $\hat{P}_0(t|k|^\beta)$  is found to be

$$\frac{\hat{P}(k, t)}{\hat{P}_0(t|k|^\beta)} \approx \begin{cases} \exp[-D_1 t |k|^{2\beta-1}] & \beta < \beta_c \\ \exp[-D_2 t k^2] & \beta > \beta_c \end{cases}, \quad (5)$$

where

$$\hat{P}_0(t|k|^\beta) = e^{-D_0 t |k|^\beta}, \quad (6)$$

with the diffusion constants  $D_0, D_1$  and  $D_2$  provided explicitly in Eq. (14). This correction, which describes the approach of  $\hat{P}(k, t)$  towards its asymptotic scaling form  $\hat{P}_0(t|k|^\beta)$ , remarkably undergoes a transition as  $\beta$  crosses  $\beta_c = 3/2$ : For  $\beta > \beta_c$ , the leading correction scales diffusively as  $|k| \propto t^{-1/2}$  while for  $\beta < \beta_c$  it remains superdiffusive, scaling as  $|k| \propto t^{-1/(2\beta-1)}$ . This transition is shown to depend only on the tail behavior of  $\phi(u)$  and is thus argued to be universal.

The analytical results presented in Eq. (5) are supplemented by numerical simulation results of the Levy walk’s dynamics (see Sec. II of the SM), denoted by  $\hat{P}_{sim}(k, t)$ , and by the exact numerical solution of Eq. (4), which is obtained via a numerical inverse-Laplace transform and denoted by  $\hat{P}_{num}(k, t)$ . Figure 2 shows the spreading of the logarithm of the Fourier-space probability density at long-times and small  $|k|$  (i.e. large distances) for  $\beta = \beta_c - \frac{1}{6} = 4/3$  and for  $\beta = \beta_c + \frac{1}{6} = 5/3$ . Numerical simulation data  $\hat{P}_{sim}(k, t)$  is presented alongside the exact numerical solution  $\hat{P}_{num}(k, t)$ , the

theoretical prediction  $\hat{P}(k, t)$  of Eq. (5) and the asymptotic solution  $\hat{P}_0(t|k|^\beta)$  of Eq. (6). To better observe the leading correction, Fig. 3 follows with a plot of  $\log[\hat{P}_{sim}(k, t)/\hat{P}_0(t|k|^\beta)]$  for large  $t$ , illustrating an excellent agreement between theory and both simulation and numerical results. The velocity magnitude and minimal walk time were set to  $v = t_0 = 1$  in the simulations and numerical solution.

*Asymptotic Analysis* - To obtain the leading correction to the asymptotic scaling solution, our strategy will be to study  $\tilde{P}(k, s)$  in the following order of limits: We first retrieve the leading behavior of  $\tilde{P}(k, s)$  for small  $s$  (i.e. large  $t$ ), then take the inverse Laplace transform and finally extract the leading correction to  $\hat{P}_0(t|k|^\beta)$  in the scaling limit  $|k| \rightarrow 0, t \rightarrow \infty$  with  $t|k|^\beta \sim const.$  As a first step, we conveniently transform to the dimensionless variables

$$\sigma = t_0 s; \quad \tau = t/t_0; \quad q = \ell_0 k, \quad (7)$$

where  $\ell_0 = t_0 v$  denotes the typical length-scale of the model. As demonstrated in Sec. III of the SM, only the leading term in the expansion of  $\tilde{\psi}(\sigma - iq) + \tilde{\psi}(\sigma + iq)$  of Eq. (4) in small  $\sigma$  and  $|q|$  enters the leading correction. This agrees with intuition, as  $\psi(t)$  in Eq. (2) for  $P(x, t)$  describes the walker's probability of arriving at  $x$  at time  $t$  during its initial excursion. Naturally, this process becomes irrelevant in our scaling regime as  $|x|$  and  $t$  grow larger.

We next consider the small  $\sigma$  behavior of  $\tilde{\phi}(\sigma \mp iq)$ , which appear in the denominator of Eq. (4). Expanding the Laplace transform in small  $\sigma$  yields

$$\tilde{\phi}(\sigma \mp iq) \approx \int_0^\infty \mathbf{d}\tau \phi(\tau) e^{\pm iq\tau} (1 - \sigma\tau), \quad (8)$$

where higher order terms of  $\mathcal{O}(\sigma^2)$  are discarded. With this, the large time behavior of  $\tilde{P}(q, \sigma)$  is recovered as

$$\tilde{P}(q, \sigma) \approx \frac{\beta}{\beta - 1} \frac{1}{A(q) + B(q)\sigma}. \quad (9)$$

To proceed, we take the inverse Laplace transform of  $\tilde{P}(q, \sigma)$  and find

$$\hat{P}(q, \tau) \approx \left( \frac{\beta}{\beta - 1} \frac{1}{B(q)} \right) e^{-I(q)\tau}. \quad (10)$$

Here we have defined

$$I(q) = \frac{A(q)}{B(q)}, \quad (11)$$

where the functions  $A(q)$  and  $B(q)$  given by

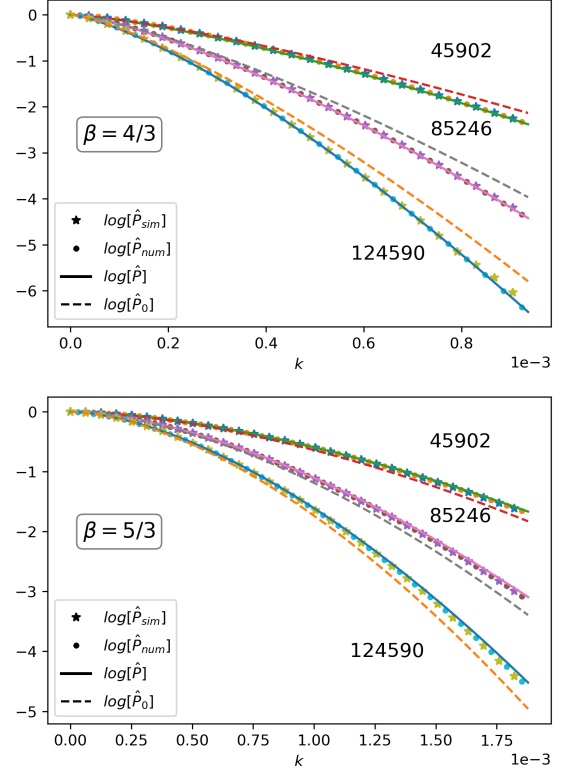


Figure 2. A log-plot of the probability density for small  $|k|$  and long-times (times are indicated near the curves). Stars denote simulation data  $\hat{P}_{sim}(k, t)$ , dots denote the numerical solution  $\hat{P}_{num}(k, t)$ , solid curves denote  $\hat{P}(k, t)$  and the dashed curves denote the asymptotic solution  $\hat{P}_0(t|k|^\beta)$ .

$$\begin{aligned} A(q) &= 1 - \langle \cos[qu] \rangle_u \approx a|q|^\beta - \frac{\beta q^2}{2(2-\beta)} + \mathcal{O}(q^4) \\ B(q) &= \partial_q \langle \sin[qu] \rangle_u \approx \frac{\beta}{\beta-1} + b|q|^{\beta-1} + \mathcal{O}(q^2), \end{aligned} \quad (12)$$

and the constants  $a$  and  $b$  respectively given by  $a = \cos\left[\frac{\pi\beta}{2}\right] \Gamma[1-\beta]$  and  $b = \beta \sin\left[\frac{\pi\beta}{2}\right] \Gamma[1-\beta]$ . We have also used  $\langle f(q, u) \rangle_u = \int_0^\infty \mathbf{d}u \phi(u) f(q, u)$  to denote the expectation value and  $\Gamma[x]$  to denote the Euler gamma function.

The long-time behavior of  $\hat{P}(q, \tau)$  finally emerges: Upon defining the scaling variable  $|z| = \tau|q|^\beta$  and taking the scaling limit  $q \rightarrow 0$  and  $\tau \rightarrow \infty$  we first note that the prefactor  $\frac{\beta}{\beta-1} \frac{1}{B(q)}$  in Eq. (10) simply reduces to unity. Next, in the same equation, observe that the expression  $I(q)\tau$  becomes

$$\frac{\beta-1}{\beta} a|z| - \frac{\beta-1}{2(2-\beta)} |z|^{\frac{2}{\beta}} \tau^{-\frac{2-\beta}{\beta}}$$

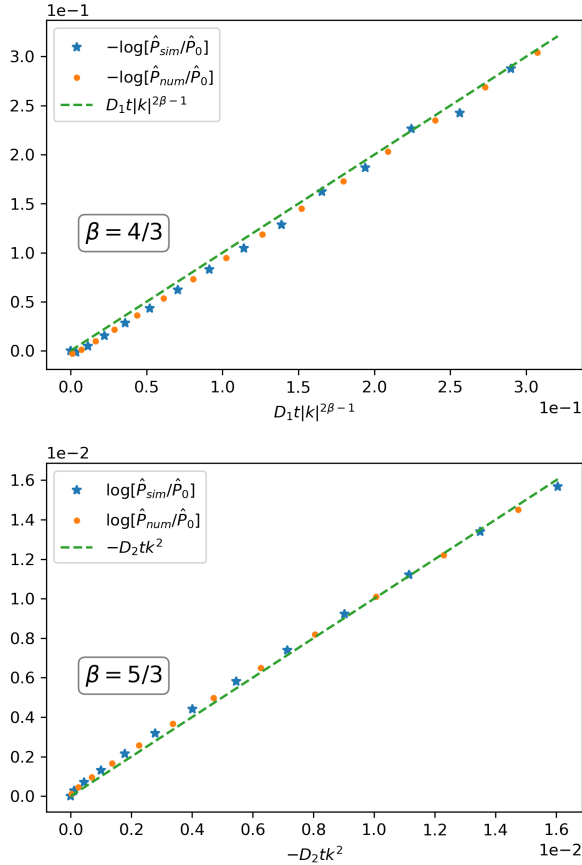


Figure 3. A log-plot for a large time ( $t \approx 4 \times 10^7$ ) of the probability density divided by the asymptotic solution versus  $D_1 t |k|^{2\beta-1}$  and  $-D_2 t k^2$  for  $\beta = 4/3$  and  $\beta = 5/3$  respectively. Blue stars denote simulation data  $\hat{P}_{sim}(k, t)$ , orange dots denote the numerical solution  $\hat{P}_{num}(k, t)$  and the dashed green curve is a linear curve provided as a guide for the eye.

$$-\left(\frac{\beta-1}{\beta}\right)^2 ab |z|^{\frac{2\beta-1}{\beta}} \tau^{-\frac{\beta-1}{\beta}}, \quad (13)$$

where faster decaying terms of  $\mathcal{O}\left(\tau^{-\frac{\beta+1}{\beta}}\right)$  are neglected. Reinstating  $(q, \tau)$  in place of  $z$  and replacing the dimensionless variables  $(q, \tau)$  by the original dimensional variables  $(k, t)$  (see Eq. (7)) yields the announced results for  $\hat{P}(k, t)$  in Eq. (5) with the diffusion coefficients  $D_0$ ,  $D_1$  and  $D_2$  given by

$$\begin{cases} D_0 = a(\beta-1)\ell_0^\beta/\beta t_0 \\ D_1 = -ab(\beta-1)^2\ell_0^{2\beta-1}/\beta^2 t_0 \\ D_2 = (\beta-1)\ell_0^2/2(\beta-2)t_0 \end{cases} \quad (14)$$

*Universality of  $\beta_c$*  - We next argue that the transition at  $\beta_c = 3/2$  follows directly from the tail behavior of

the walk-time distribution and is thus universal. To this end, let us retrace our steps and take a second look at the derivation of  $\hat{P}(q, \tau)$ . In Eq. (10), we have found that the large-time behavior of  $\hat{P}(q, \tau)$  is determined by  $I(q)$ . Since the walk-time  $u$  is non-negative, any choice of a walk-time distribution must vanish for non-positive values of  $u$ . Thus, the integration range in the expectation integrals  $\langle \cos[qu] \rangle_u$  and  $\langle \sin[qu] \rangle_u$  of Eq. (12) for  $A(q)$  and  $B(q)$  can be safely extended to  $u \in (-\infty, +\infty)$ . The function  $I(q)$  can then be expressed in terms of the characteristic function of  $\phi(u)$ ,  $\hat{\phi}(\pm q) = \int_{-\infty}^{\infty} \mathbf{d}u \phi(u) e^{\mp iqu}$ , such that

$$I(q) = \frac{1 - \text{Re} \left[ \hat{\phi}(q) \right]}{\partial_q \text{Im} \left[ \hat{\phi}(q) \right]}, \quad (15)$$

where we have used the Hermitian property of the characteristic function  $\hat{\phi}(-q) = \hat{\phi}(q)^*$ .

We are now at a good vantage point to hold a more general discussion on the structure of  $I(q)$ . Since the walk-time distribution is one-sided, it is non-symmetric so its Fourier transform  $\hat{\phi}(q)$  contains both real and imaginary terms. Now, had all of the moments of  $\phi(u)$  been finite,  $\hat{\phi}(q)$  would have been an analytic function whose power series expansion about  $q \rightarrow 0$  has the  $n^{\text{th}}$  order coefficient  $\propto (i)^n \langle u^n \rangle_u$ . However, due to its heavy tail, the moments of  $\phi(u)$  are not all finite and additional non-analytic terms must also appear in  $\hat{\phi}(q)$ . Indeed, it is straightforward to show that a heavy tail  $\propto u^{-1-\beta}$  in  $\phi(u)$  results in real and imaginary non-analytic terms in  $\hat{\phi}(q)$  which are  $\propto |q|^\beta$ . The characteristic function  $\hat{\phi}(q)$  is thus the sum of two parts, each containing of both real and imaginary terms: The first being an analytic power series in  $q$  while the second is a non-analytic contribution  $\propto |q|^\beta$ , i.e.  $\hat{\phi}(q) = \text{Re} \left[ \hat{\phi}(q) \right] + i \text{Im} \left[ \hat{\phi}(q) \right]$  with

$$\begin{cases} \text{Re} \left[ \hat{\phi}(q) \right] = \sum_{n=0}^{\infty} c_{2n} q^{2n} + d_1 |q|^\beta \\ \text{Im} \left[ \hat{\phi}(q) \right] = \sum_{n=0}^{\infty} c_{2n+1} q^{2n+1} + d_2 |q|^\beta \end{cases}, \quad (16)$$

where  $c_n$  are  $q$ -independent coefficients with  $d_1$  and  $d_2$  possibly depending on the sign of  $q$ . Although Eq. (16) already sheds some light on  $I(q)$ , we can go a step further by employing a few general properties of  $\hat{\phi}(q)$ . Since  $\hat{\phi}(q)$  is the Fourier transform of a normalized distribution, its value at  $q = 0$  sets the coefficient  $c_0 = 1$ . Next, the coefficient  $c_1$  is set by the first moment of  $\phi(u)$ , which is finite for any  $1 < \beta < 2$ . Lastly,  $c_2$  is set by the second moment of the analytic part of  $\hat{\phi}(q)$ , which describes the small  $u$  behavior of  $\phi(u)$ , i.e. the

complementary of its large  $u$  tail behavior. Following this reasoning, we approximate  $I(q)$  for small  $|q|$  by

$$I(q) \approx \frac{d_1 |q|^\beta + c_2 q^2}{c_1 + \beta d_2 |q|^{\beta-1}}, \quad (17)$$

which has the same form as in Eqs. (12), (13) which led to a transition in the leading behavior of  $\hat{P}(k, t) / \hat{P}_0(t | k|^\beta)$  at  $\beta = \beta_c$ . However, here this transition was obtained under quite general considerations, namely that  $\phi(u)$  has a heavy tail  $\propto u^{-1-\beta}$ , and is thus argued to be universal. Section IV of the SM explicitly presents  $\hat{\phi}(q)$  for our particular choice of  $\phi(u)$  in Eq. (1), showing it to be in full agreement with Eq. (16).

*Conclusions* - In this letter, the leading correction to the asymptotic scaling solution of the probability density was studied for a Levy walk of order  $1 < \beta < 2$ . This correction, which describes the model's approach towards its asymptotic form, was shown to undergo a transition in which its scaling remarkably changes from simple diffusion to superdiffusion as  $\beta$  crosses the critical value  $\beta_c = 3/2$ . The transition was shown to depend only on the tail behavior of the walk time distribution and was thus argued to be universal.

The robustness of these results suggest they could help researchers detect and confirm superdiffusive behavior in different systems for which the asymptotic limit is hard to reach. In such systems, finite space-time corrections are often vital for reliably identifying and determining their anomalous properties, both under equilibrium and non-equilibrium settings. For example, one field in which such corrections are well known to pose a significant challenge is the study of anomalous

heat transport [3, 6–8, 24, 30, 31]. In [3], the Levy walk of order  $\beta = 5/3$  was used to model the asymptotic superdiffusive spreading of energy perturbations and entailing anomalous transport properties of a particular 1d gas model. There, the authors stress the great difficulty imposed by such corrections. Nevertheless, relying on general hydrodynamical arguments, the connection to the Levy walk model was suggested to extend to a class of similar models [3]. Indeed, a diffusive correction to the energy spreading, and a corresponding “normal” correction to the heat current, have recently been reported in a different 1d gas model [31]. Similarly, a normal diffusive correction to the anomalous stationary current was rigorously derived for the 1d Levy walk of order  $\beta > 3/2$  under nonequilibrium settings in [8]. Both of these results are consistent with, and provide support for, the findings reported in this letter. It would thus be of interest to test these results in additional experimental and numerical setups which are effectively modeled by the Levy walk, especially ones in which  $\beta < \beta_c$ . It would also be interesting to study the onset of superdiffusion in the closely related Levy flight model where, rather than drawing a walk time and moving at a finite velocity for that duration, particles instead draw a flight distance and immediately materialize at their new position [21, 32, 33].

*Acknowledgments* - I thank David Mukamel for his ongoing encouragement and support, as well as for many helpful discussions. I also thank Hillel Aharony, Julien Cividini, Anupam Kundu, Bertrand Lacroix-A-Chez-Toine and Oren Raz for a critical reading of this manuscript and for their helpful remarks. This work was supported by a research grant from the Center of Scientific Excellence at the Weizmann Institute of Science.

- 
- [1] MF Shlesinger, BJ West, and Joseph Klafter. Lévy dynamics of enhanced diffusion: Application to turbulence. *Physical Review Letters*, 58(11):1100, 1987.
  - [2] Ori Saporta Katz and Efi Efrati. Self-driven fractional rotational diffusion of the harmonic three-mass system. *Physical review letters*, 122(2):024102, 2019.
  - [3] P Cipriani, S Denisov, and A Politi. From anomalous energy diffusion to levy walks and heat conductivity in one-dimensional systems. *Physical review letters*, 94(24):244301, 2005.
  - [4] V Zaburdaev, S Denisov, and Peter Hänggi. Perturbation spreading in many-particle systems: a random walk approach. *Physical review letters*, 106(18):180601, 2011.
  - [5] Sha Liu, XF Xu, RG Xie, Gang Zhang, and BW Li. Anomalous heat conduction and anomalous diffusion in low dimensional nanoscale systems. *The European Physical Journal B*, 85(10):337, 2012.
  - [6] Abhishek Dhar, Keiji Saito, and Bernard Derrida. Exact solution of a lévy walk model for anomalous heat transport. *Physical Review E*, 87(1):010103, 2013.
  - [7] Julien Cividini, Anupam Kundu, Asaf Miron, and David Mukamel. Temperature profile and boundary conditions in an anomalous heat transport model. *Journal of Statistical Mechanics: Theory and Experiment*, 2017(1):013203, 2017.
  - [8] Asaf Miron. Lévy walks on finite intervals: A step beyond asymptotics. *Phys. Rev. E*, 100:012106, Jul 2019.
  - [9] P Levitz. From knudsen diffusion to levy walks. *EPL (Europhysics Letters)*, 39(6):593, 1997.
  - [10] Dirk Brockmann and Theo Geisel. Lévy flights in inhomogeneous media. *Physical review letters*, 90(17):170601, 2003.

- [11] S Marksteiner, K Ellinger, and P Zoller. Anomalous diffusion and lévy walks in optical lattices. *Physical Review A*, 53(5):3409, 1996.
- [12] Hidetoshi Katori, Stefan Schlipf, and Herbert Walther. Anomalous dynamics of a single ion in an optical lattice. *Physical Review Letters*, 79(12):2221, 1997.
- [13] Yoav Sagi, Miri Brook, Ido Almog, and Nir Davidson. Observation of anomalous diffusion and fractional self-similarity in one dimension. *Physical review letters*, 108(9):093002, 2012.
- [14] Andy M Reynolds. Current status and future directions of lévy walk research. *Biology open*, 7(1):bio030106, 2018.
- [15] A. Ott, J. P. Bouchaud, D. Langevin, and W. Urbach. Anomalous diffusion in “living polymers”: A genuine lévy flight? *Phys. Rev. Lett.*, 65:2201–2204, Oct 1990.
- [16] Sergey V. Buldyrev, Ary L. Goldberger, Shlomo Havlin, Chung-Kang Peng, Michael Simons, and H. Eugene Stanley. Generalized lévy-walk model for dna nucleotide sequences. *Phys. Rev. E*, 47:4514–4523, Jun 1993.
- [17] Arpita Upadhyaya, Jean-Paul Rieu, James A Glazier, and Yasuji Sawada. Anomalous diffusion and non-gaussian velocity distribution of hydra cells in cellular aggregates. *Physica A: Statistical Mechanics and its Applications*, 293(3-4):549–558, 2001.
- [18] Injong Rhee, Minsu Shin, Seongik Hong, Kyunghan Lee, Seong Joon Kim, and Song Chong. On the lévy-walk nature of human mobility. *IEEE/ACM transactions on networking (TON)*, 19(3):630–643, 2011.
- [19] David A Raichlen, Brian M Wood, Adam D Gordon, Audax ZP Mabulla, Frank W Marlowe, and Herman Pontzer. Evidence of lévy walk foraging patterns in human hunter–gatherers. *Proceedings of the National Academy of Sciences*, 111(2):728–733, 2014.
- [20] Michael F Shlesinger, Joseph Klafter, and YM Wong. Random walks with infinite spatial and temporal moments. *Journal of Statistical Physics*, 27(3):499–512, 1982.
- [21] V Zaburdaev, S Denisov, and J Klafter. Lévy walks. *Reviews of Modern Physics*, 87(2):483, 2015.
- [22] G Zumofen and J Klafter. Scale-invariant motion in intermittent chaotic systems. *Physical Review E*, 47(2):851, 1993.
- [23] SV Buldyrev, S Havlin, A Ya Kazakov, MGE Da Luz, EP Raposo, HE Stanley, and GM Viswanathan. Average time spent by lévy flights and walks on an interval with absorbing boundaries. *Physical Review E*, 64(4):041108, 2001.
- [24] S Denisov, J Klafter, and M Urbakh. Dynamical heat channels. *Physical review letters*, 91(19):194301, 2003.
- [25] Andrew M Edwards, Richard A Phillips, Nicholas W Watkins, Mervyn P Freeman, Eugene J Murphy, Vsevolod Afanasyev, Sergey V Buldyrev, Marcos GE da Luz, Ernesto P Raposo, H Eugene Stanley, et al. Revisiting lévy flight search patterns of wandering albatrosses, bumblebees and deer. *Nature*, 449(7165):1044, 2007.
- [26] David W Sims, David Righton, and Jonathan W Pitchford. Minimizing errors in identifying lévy flight behaviour of organisms. *Journal of Animal Ecology*, 76(2):222–229, 2007.
- [27] Simon Benhamou. How many animals really do the lévy walk? *Ecology*, 88(8):1962–1969, 2007.
- [28] Marta C Gonzalez, Cesar A Hidalgo, and Albert-Laszlo Barabasi. Understanding individual human mobility patterns. *nature*, 453(7196):779, 2008.
- [29] Tajie H Harris, Edward J Banigan, David A Christian, Christoph Konradt, Elia D Tait Wojno, Kazumi Norose, Emma H Wilson, Beena John, Wolfgang Weninger, Andrew D Luster, et al. Generalized lévy walks and the role of chemokines in migration of effector cd8+ t cells. *Nature*, 486(7404):545, 2012.
- [30] Stefano Lepri. *Thermal transport in low dimensions: from statistical physics to nanoscale heat transfer*, volume 921. Springer, 2016.
- [31] Asaf Miron, Julien Cividini, Anupam Kundu, and David Mukamel. Derivation of fluctuating hydrodynamics and crossover from diffusive to anomalous transport in a hard-particle gas. *Physical Review E*, 99(1):012124, 2019.
- [32] Michael F Shlesinger and Joseph Klafter. Lévy walks versus lévy flights. In *On growth and form*, pages 279–283. Springer, 1986.
- [33] Alexander A Dubkov, Bernardo Spagnolo, and Vladimir V Uchaikin. Lévy flight superdiffusion: an introduction. *International Journal of Bifurcation and Chaos*, 18(09):2649–2672, 2008.

**SUPPLEMENTAL MATERIAL -  
UNIVERSALITY IN THE ONSET OF  
SUPER-DIFFUSION IN LEVY WALKS**

**I. FOURIER-LAPLACE TRANSFORM OF EQ. (2)**

The derivation of Eq. (4) of the main text for the Fourier-Laplace transformed probability density  $\tilde{P}(k, s)$  is presented, starting from Eq. (2) which describes the walker's position probability density  $P(x, t)$ , i.e.

$$P(x, t) = \frac{\psi(t)}{2} \delta(|x| - vt)$$

$$+ \frac{1}{2} \int_0^t \mathbf{d}u \phi(u) [P(x - vu, t - u) + P(x + vu, t - u)].$$

We first Fourier transform the equation and obtain

$$\begin{aligned} \hat{P}(k, t) &= \psi(t) \cos(ktv) \\ + \frac{1}{2} \int_0^t \mathbf{d}u \phi(u) &\left[ \int_{-\infty}^{\infty} \mathbf{d}z e^{ik(z+vu)} P(z, t-u) \right. \\ &\left. + \int_{-\infty}^{\infty} \mathbf{d}z e^{ik(z-vu)} P(z, t-u) \right] \\ &= \psi(t) \cos(ktv) \\ &+ \int_0^t \mathbf{d}u \phi(u) \hat{P}(k, t-u) \cos(kvu), \end{aligned} \quad (18)$$

where  $\hat{P}(k, t) = \int_{-\infty}^{\infty} \mathbf{d}x e^{ikx} P(x, t)$  was used. We next follow with a Laplace transform which yields

$$\begin{aligned} \tilde{P}(k, s) &= \frac{1}{2} \left( \int_0^{\infty} \mathbf{d}t e^{-t(s-ikv)} \psi(t) \right. \\ &+ \left. \int_0^{\infty} \mathbf{d}t e^{-t(s+ikv)} \psi(t) \right) + \frac{1}{2} \int_0^{\infty} \mathbf{d}t e^{-st} \\ &\times \int_0^t \mathbf{d}u \phi(u) \hat{P}(k, t-u) (e^{ikuv} + e^{-ikuv}) \\ &= \frac{1}{2} [\tilde{\psi}(s-ikv) + \tilde{\psi}(s+ikv)] \\ &+ \frac{1}{2} \tilde{P}(k, s) [\tilde{\phi}(s-ikv) + \tilde{\phi}(s+ikv)], \end{aligned} \quad (19)$$

where  $\tilde{P}(k, s) = \int_0^{\infty} \mathbf{d}t e^{-st} \hat{P}(k, t)$  was used. Isolating  $\tilde{P}(k, s)$  then gives Eq. (4) of the main text, i.e.

$$\tilde{P}(k, s) = \frac{\tilde{\psi}(s-ikv) + \tilde{\psi}(s+ikv)}{2 - \tilde{\phi}(s-ikv) - \tilde{\phi}(s+ikv)}.$$

**II. SIMULATION PROCEDURE**

To obtain the simulated walker probability density in Fourier space  $\hat{P}_{sim}(k, t)$ , which appears in Figures 2, 3 of the main text, the following procedure was carried out. Each walker was initialized at the origin of the interval  $[-\frac{L}{2}, +\frac{L}{2}]$  with a velocity of magnitude  $v = 1$  pointing towards a random direction  $\pm 1$  and a walk time  $u$  drawn from the walk time distribution  $\phi(u)$  of Eq. (1) of the main text. In each realization the Levy walk dynamics ran up to time  $T = 0.45(L/v)$  to ensure the walker could not escape the interval. During this time, the interval was divided into bins of size  $\Delta x$  and at each time interval  $\Delta t$  the walker's position  $X(t)$  was mapped onto the appropriate bin  $x_m = [m\Delta x, (m+1)\Delta x]$ , where  $m = 1, 2, \dots, M$  and  $M = \frac{L}{\Delta x} \in \mathbb{N}$ . By repeating this procedure for  $\sim 10^7$  realization, a histogram for the probability  $P(x_m, t_n)$  of finding the walker at bin  $x_m$  at time  $t_n = n\Delta t$  was obtained, where  $n = 1, 2, \dots, N$  with  $N = \frac{T}{\Delta t}$ . Finally,  $\hat{P}_{sim}(k_m, t_n)$  was obtained by taking a Fourier transform of  $P(x_m, t_n)$ , with  $k_m$  given by  $k_m = \frac{2\pi m}{L}$ .

**III. EXPANSION OF  $\tilde{\psi}(\sigma - iq) + \tilde{\psi}(\sigma + iq)$**

We here show that only the leading term in the expansion of  $\tilde{\psi}(\sigma - iq) + \tilde{\psi}(\sigma + iq)$  in small  $\sigma$  and  $|q|$  (i.e. large times and distances), which appears in the numerator of Eq. (4) of the main text, is relevant when computing the leading correction to  $\hat{P}_0(\tau |q|^\beta)$ . As in the calculation of  $\tilde{\phi}(\sigma \pm iq)$  of Eq. (8) in the main text, we first consider long times and expand in small  $\sigma$

$$\begin{aligned} &\tilde{\psi}(\sigma - iq) + \tilde{\psi}(\sigma + iq) \\ &\approx 2 \left[ \int_0^{\infty} \mathbf{d}\tau \psi(\tau) \cos[q\tau] \right. \\ &\quad \left. - \partial_q \left( \int_0^{\infty} \mathbf{d}\tau \psi(\tau) \sin[q\tau] \right) \sigma \right], \end{aligned} \quad (20)$$

where corrections of order  $\mathcal{O}(\sigma^2)$  are neglected. For small  $|q|$  this becomes

$$\begin{aligned} &\tilde{\psi}(\sigma - iq) + \tilde{\psi}(\sigma + iq) \approx m + n |q|^{\beta-1} \\ &+ pq^2 - \left( r - w |q|^{\beta-2} + zq^2 \right) \sigma + \mathcal{O}(q^3), \end{aligned} \quad (21)$$

where

$$\begin{cases} m = \frac{2\beta}{\beta-1} ; & n = 2 \sin \left[ \frac{\pi\beta}{2} \right] \Gamma [1 - \beta] \\ p = \frac{\beta}{3(3-\beta)} ; & r = \frac{\beta}{\beta-2} \\ w = 2 \cos \left[ \frac{\pi\beta}{2} \right] \Gamma [2 - \beta] ; & z = \frac{\beta}{4(4-\beta)} \end{cases} . \quad (22)$$

Repeating this for  $2 - \tilde{\phi}(\sigma - iq) - \tilde{\phi}(\sigma + iq)$  in the denominator of Eq. (4) of the main text, yields

$$2 - \tilde{\phi}(\sigma - iq) - \tilde{\phi}(\sigma + iq)$$

$$\approx G |q|^\beta + Hq^2 + \sigma \left( J + M |q|^{\beta-1} + Pq^2 \right) + \mathcal{O}(q^3), \quad (23)$$

with the constants

$$\begin{cases} G = 2 \cos \left[ \frac{\pi\beta}{2} \right] \Gamma [1 - \beta] ; & H = \frac{\beta}{\beta-2} \\ J = \frac{2\beta}{\beta-1} ; & M = 2\beta \sin \left[ \frac{\pi\beta}{2} \right] \Gamma [1 - \beta] \\ P = \frac{\beta}{3-\beta} \end{cases} . \quad (24)$$

Substituting both  $\tilde{\psi}(\sigma - iq) + \tilde{\psi}(\sigma + iq)$  and  $2 - \tilde{\phi}(\sigma - iq) - \tilde{\phi}(\sigma + iq)$  into Eq. (4) of the main text gives

$$\tilde{P}(q, \sigma) \approx \frac{m + n |q|^{\beta-1} + pq^2 - \left( r - w |q|^{\beta-2} + zq^2 \right) \sigma}{G |q|^\beta + Hq^2 + \sigma \left( J + M |q|^{\beta-1} + Pq^2 \right)}. \quad (25)$$

To justify replacing the numerator  $\tilde{\psi}(\sigma - iq) + \tilde{\psi}(\sigma + iq)$  by its leading correction  $m$ , the leading terms in the expansion of  $\tilde{P}(q, \sigma)$  must be shown to be independent of all of the other coefficients appearing in Eq. (22) (i.e. the coefficients denoted by lower-case letters),

to  $\mathcal{O}(\sigma)$  for small  $|q|$ . A straightforward calculation verifies this is indeed the case.

#### IV. HYPERGEOMETRIC FUNCTIONS AS POWER SERIES

For our choice of  $\phi(u)$  in Eq. (1) of the main text, the characteristic function  $\hat{\phi}(q)$  is given by

$$\hat{\phi}(q) = f(q; \beta) - i \frac{\beta}{\beta-1} qg(q; \beta)$$

$$+ \beta \Gamma [-\beta] \left( \cos \left[ \frac{\pi\beta}{2} \right] + i \sin \left[ \frac{\pi\beta}{2} \right] \text{sgn}[q] \right) |q|^\beta. \quad (26)$$

The first line contains

$$\begin{cases} f(q; \beta) := {}_1F_2 \left[ \left\{ -\frac{\beta}{2} \right\}; \left\{ \frac{1}{2}, \frac{2-\beta}{2} \right\}; -\frac{q^2}{4} \right] \\ g(q; \beta) := {}_1F_2 \left[ \left\{ \frac{1-\beta}{2} \right\}; \left\{ \frac{3}{2}, \frac{3-\beta}{2} \right\}; -\frac{q^2}{4} \right] \end{cases}, \quad (27)$$

which are generalized hypergeometric functions. These can be represented by the power series

$${}_pF_q \left[ \{a_i\}_{i=1}^p; \{b_j\}_{j=1}^q; z \right] = \sum_{n=0}^{\infty} \frac{(a_1)_n \dots (a_p)_n z^n}{(b_1)_n \dots (b_q)_n n!}, \quad (28)$$

where the Pochhammer symbol  $(y)_n$  is given by

$$(y)_n = \frac{\Gamma[y+n]}{\Gamma[y]} \quad (29)$$

and  $\Gamma[x]$  is the Gamma function. Thus,  $f(q; \beta)$  and  $g(q; \beta)$  are simply compact notations for convergent power series in  $q$ . As argued in the main text, these describe the analytic contributions to  $\hat{\phi}(q)$ . On the other hand, the second line of Eq. (26) contains non-analytic terms  $\propto |q|^\beta$  which are due to the heavy tail of  $\phi(u)$ .